

Phase-locked, low-noise, frequency agile titanium:sapphire lasers for simultaneous atom interferometers

Holger Müller, Sheng-wei Chiow, Quan Long, and Steven Chu

Department of Physics, Stanford University, Stanford, California 94305-4060

Received July 27, 2005; revised October 6, 2005; accepted October 10, 2005

We demonstrate a laser system consisting of a >1.6 W titanium:sapphire laser that is phase locked to another free-running titanium:sapphire laser at a wavelength of 852 nm with a phase noise of -138 dBc/Hz at 1 MHz from the carrier, using an intracavity electro-optic phase modulator. The residual phase variance is 2.5×10^{-8} rad² integrated from 1 Hz to 10 kHz. This system can phase-continuously change the offset frequency within 200 ns with frequency steps up to 4 MHz. Simultaneous atom interferometers can make full use of this ultralow phase noise in differential measurements, where influences from the vibration of optics are greatly suppressed in common mode. © 2006 Optical Society of America
OCIS codes: 120.0120, 020.0020, 120.5050.

The ability to precisely stabilize and manipulate the frequency and phase of laser light is at the basis of tremendous progress in precision measurements, including the realization of optical clocks^{1,2} and tests of the fundamental laws of physics.³ This ability has been extended to phase-locking femtosecond lasers.⁴ Low-noise phase-locked continuous-wave (cw) lasers are also extensively used for cooling, condensing, and manipulating atoms,⁵ and in particular, atom interferometry is used in sensitive gyroscopes, precision gravimeters and gravity gradiometers, and precision measurements of fundamental constants.⁶ In these applications, laser light serves as a reference for measuring the phase evolution of the matter waves. Thus lasers with ultralow phase noise are required to achieve present atom interferometer accuracy goals.

To achieve low phase noise, fast feedback mechanisms are necessary to efficiently remove the frequency or phase fluctuations of the laser emission. In such atom-manipulation systems, extended cavity diode lasers are widely used, because their output frequencies and phases can be easily controlled by changing the injection current. Other than using fast feedback, low-noise phase locking in diode laser systems can also be obtained by injection locking.⁷ For Nd:YAG lasers, which have an intrinsically small linewidth, the performance of cw phase-locked lasers can reach -125 dBc/Hz at 10 Hz offset from the carrier.⁸

In addition to ultralow phase noise, applications in atomic physics often require high optical power and fast (microseconds), precise steps in frequency (frequency agility).⁹ Although delicate phase-locked diode lasers can be frequency agile, these diode laser systems with an optical power of higher than 1 W are rare, even with the help of commercially available optical power amplifiers. Haubrich and Wynands achieved phase locking of a Ti:sapphire laser to a stable diode laser of 4 kHz linewidth with a phase noise of approximately -90 dBc/Hz at 1 MHz offset by use of an intracavity electro-optic phase modulator (EOM).¹⁰ Here we demonstrate a cw phase-locked system of two Ti:sapphire lasers, each providing

more than 1.6 W output power, with a phase noise of -138 dBc/Hz at 1 MHz from the carrier. Our system can achieve phase-continuous frequency steps of 4 MHz in 200 ns.

Both master and slave lasers are Coherent 899-21 Ti:sapphire ring lasers in the high-power-pump configuration with control boxes modified as suggested by Haubrich and Wynands.¹⁰ The master laser is pumped with 10.5 W from a Coherent Verdi-10. The frequency of the master laser is stabilized to its reference cavity with supplied servo elements and electronics, and the single-frequency output power is 1.6 W at 852 nm. The master laser can be free running but will be referenced to a Cs vapor cell for frequency stability in our future applications. The slave laser is pumped by a Coherent Innova 400-15 argon-ion laser with 19 W multiline output power. An EOM (Linios PM25IR) is inserted into the resonator between the Faraday rotator and the upper fold mirror. This causes the output power to drop by $\sim 20\%$ to 1.85 W. For locking, optical power is picked up from each Ti:sapphire laser by using a residual reflection from a common optical element. A total of 2 mW reaches the beat detector (Fig. 1). The beat note is amplified and a double-balanced mixer (DBM) serves as a phase detector, with the local oscillator (LO) input driven by an Agilent E8241A synthesizer at ~ 168 MHz. To prevent laser amplitude fluctuations from coupling into the phase noise measurement, a

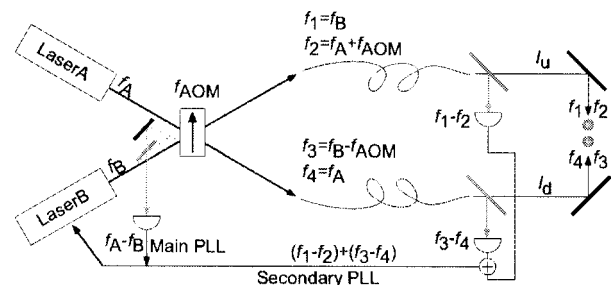


Fig. 1. Frequency generation and phase-locking scheme for simultaneous atom interferometers. AOM, acousto-optic modulator.

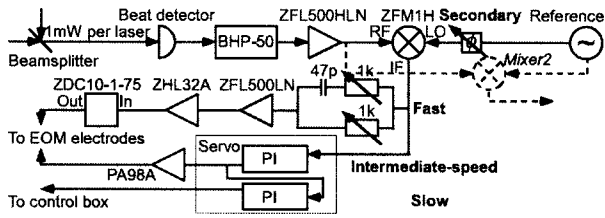


Fig. 2. Feedback loop block diagram.

50 MHz high-pass filter is placed before the phase detector.

The feedback to the slave laser consists of three paths: a slow, an intermediate-speed, and a fast path (Fig. 2). The slow feedback path has a proportional-integral (PI) control with a bandwidth of 20 kHz. It controls the length of the laser's resonant cavity through the modified control box, which modulates a piezoactuated mirror and etalons in the cavity. The fast and the intermediate-speed feedback paths feed to opposite electrodes of the intracavity EOM. The intermediate-speed path uses a PI controller (Fig. 3) and a high-voltage operational amplifier (Apex PA98A, with a high slew rate of $1000 \text{ V}/\mu\text{s}$ and $\pm 150 \text{ V}$ swing) for driving the EOM, which provides a frequency tuning coefficient of $0.2 \text{ MHz}/\text{V}$. The bandwidth of this path is limited to 0.8 MHz by the PA98A.¹¹ The fast feedback path consists of a passive proportional-differential (PD) controller followed by an rf power amplifier (Fig. 3). After this rf amplifier, a directional coupler is inserted before connecting to an electrode of the EOM to ground the electrode for dc voltages. The differential control in the fast path compensates for phase lag due to propagation delay at high frequencies. We achieve an overall closed-loop bandwidth of $\sim 10 \text{ MHz}$, limited by the propagation delay in the optical and electronic signal path lengths.

We study the performance of the phase-locked lasers using a separate beat detector after passing both beams through one single-mode polarization-maintaining fiber with the same polarization for an out-of-loop measurement. Figure 4 (solid curve) shows the phase noise spectral density. The wideband ($>100 \text{ kHz}$) noise, which goes down to $-138 \text{ dBc}/\text{Hz}$, is measured with an HP 8590B spectrum analyzer, and the low-frequency noise is measured with a SRS SR785 FFT signal analyzer by downconverting the beat signal to dc with a separate DBM but using the same LO as that in the phase-locked loop (PLL). (This is found to be necessary, as otherwise the measurement is limited by the noise of LO.) The peaks at 9 MHz indicate the loop bandwidth. The residual phase variance integrated over a frequency range from 1 Hz to 10 kHz is approximately 10^{-6} rad^2 (solid curve).

For comparison, we also measure the phase noise with a digital phase detector (Analog Devices AD9901) instead of a DBM (Fig. 4). The $\sim 8 \text{ dB}$ increase of the wideband phase noise probably arises from the conversion of the analog waveforms into digital signals, where voltage noise in the analog signal causes phase noise as it makes uncertain the time of zero crossings.

The frequency agility is illustrated by stepping the LO frequency. We find that with the DBM, phase lock without cycle slips is maintained for sudden phase-continuous frequency changes as large as 4 MHz . This 4 MHz frequency step is limited by the $\sim 20 \text{ Vp}$ dynamic range of the fast feedback path. The transient behavior of the PLL is examined by adding a square wave signal to the output of the DBM. The slave laser settles to 20% within 200 ns after each step.

The rise of phase noise at low frequencies (solid curve in Fig. 4) is mainly due to laser pointing fluctuations, air flow, and optics vibration. This noise is not revealed in an electronically out-of-loop measurement ($-110 \text{ dBc}/\text{Hz}$ at low frequencies, gray curve in Fig. 4) using the same photodetector but a separate mixer (Mixer2 in Fig. 2). (The best performance in this measurement is achieved by replacing the 17 dBm types ZFM-1H by 27 dBm types VAY-1, both by minicircuits.) Although this electronically out-of-loop performance is similar to the one reached by Ye and Hall,⁸ an atom interferometer still suffers the much higher noise.

This is because the two beams must be sent to the atoms via separate paths in a counterpropagating geometry. Differential vibrational noise in these paths would essentially increase the noise to the level of the solid curve in Fig. 4, even if the noise is suppressed to a lower level at one point in the setup.

We can avoid this and thus employ the ultralow phase noise of the lasers by having two simultaneous interferometers in an arrangement shown in Fig. 1. Four frequencies $f_1 \dots f_4$ are generated from the two phase-locked Ti:sapphire lasers using an acousto-optic modulator. Using atoms in different [internal and (or) external] states, the individual interferometers are addressed by the beam pairs with the frequencies $\{f_1, f_4\}$ and $\{f_2, f_3\}$, respectively. In many cases, e.g., the photon recoil measurements¹² and the gravity gradient measurements,¹³ interesting physics is revealed in the difference of the interferometer phases, which are proportional to the frequency differences $f_1 - f_4$ and $f_2 - f_3$. For effective noise reduction, we take the beat notes of overlapped beams at $f_1 - f_2$ and $f_3 - f_4$, and phase lock their sum $(f_1 - f_2) + (f_3 - f_4)$ by a secondary PLL, which is added to the main PLL by shifting the LO phase. This, however, is the frequency containing the information, $(f_1 - f_4) - (f_2 - f_3)$; thus the laser frequencies are generated such that the differential phase is directly stabilized.

Noise from vibrational variations of the optical path lengths $\delta l_u, \delta l_d$ from the beat detectors to the atoms for the upper and lower beams (Fig. 1) is effectively canceled: In the individual paths, it causes optical phase changes of $2\pi\delta l_u(f_{1,2}/c)$, $2\pi\delta l_d(f_{3,4}/c)$, which results in phase shifts in the individual atom interferometers proportional to $2\pi(\delta l_u(f_1/c) - \delta l_d(f_4/c))$ and $2\pi(\delta l_u(f_2/c) - \delta l_d(f_3/c))$. The difference of the readout phases of the simultaneous interferometers is then proportional to $2\pi(\delta l_u[(f_1 - f_2)/c] - \delta l_d[(f_4 - f_3)/c])$. Since the wavelengths of the beat-note frequencies $\lambda_{ij} = c/(f_i - f_j)$ is large compared to the

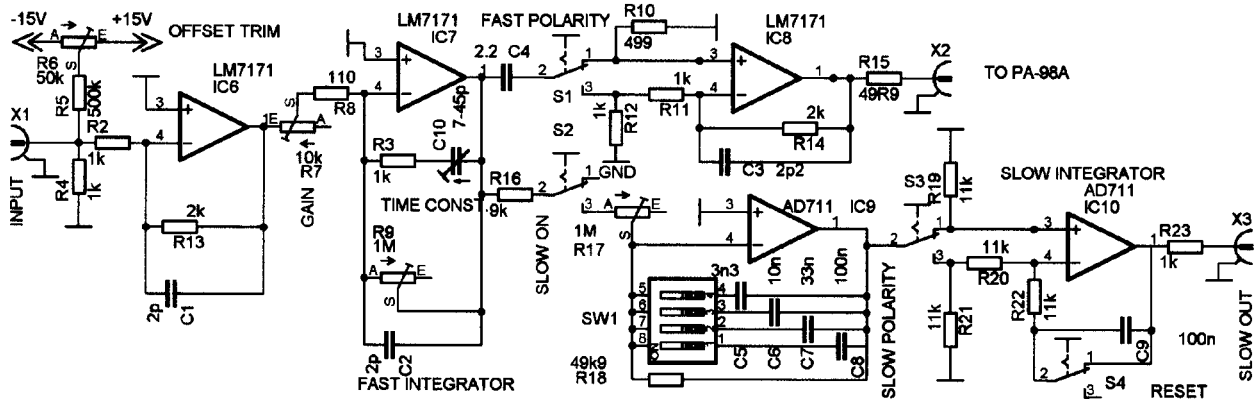


Fig. 3. Schematic of the slow and intermediate-speed PI controllers.

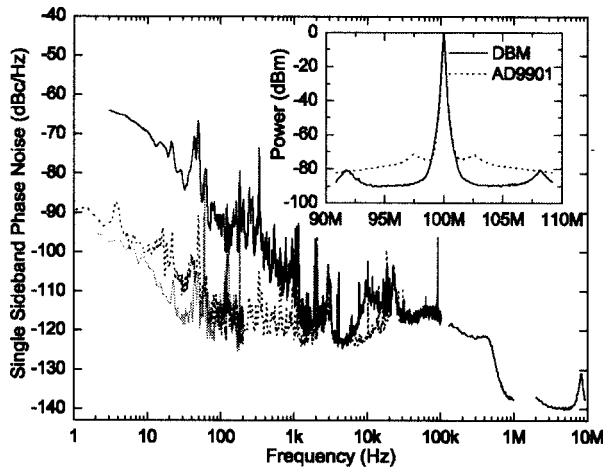


Fig. 4. Residual phase noise with an analog phase detector (measured out of loop). Solid curve, phase lock before fiber only; dashed curve: phase lock after fiber; gray curve, electronic out-of-loop phase noise measured with Mixer2 in Fig. 2. The gaps at 100 kHz and 1 MHz are due to different range settings between data sets. Inset, phase noise spectra of analog and digital phase detectors. Resolution bandwidth, 100 kHz.

amplitude of vibrations δl_u , δl_d , the common-mode noise is strongly suppressed. We operate such a secondary PLL for the differential phase (Fig. 1), and measure the residual noise in the differential phase using another beat detector at a different point in the optical path. As a result, the phase variance integrated from 1 Hz to 10 kHz (dashed curve in Fig. 4) is reduced to $2.5 \times 10^{-8} \text{ rad}^2$, which is servo gain limited.

In summary, we have demonstrated phase-locked 1.6 W Ti:sapphire lasers with an ultralow phase noise of -138 dBc/Hz at 1 MHz offset, capable of making instantaneous difference frequency steps of up to 4 MHz in 200 ns without cycle slips. We have described the use of this laser system for simulta-

neous atom interferometers. The readout of the differential phase of the interferometers can make use of this low noise; noise from optics vibrations is canceled. This will be used to perform atom interferometry for photon-recoil measurements using Cs atoms with parts-per-billion accuracy.

We thank Chris Vo for discussions. H. Müller (holgerm@stanford.edu) acknowledges support from the Alexander von Humboldt Foundation. This work is sponsored in part by grants from the Air Force Office of Scientific Research, the NSF, and the Multi-University Research Initiative. S.-w. Chiow's e-mail address is swchiow@stanford.edu

References

1. Th. Udem, R. Holzwarth, and T. W. Hänsch, *Nature* **416**, 233 (2002).
2. G. Wilpers, T. Binnewies, C. Degenhardt, U. Sterr, J. Helmcke, and F. Riehle, *Phys. Rev. Lett.* **89**, 230801 (2002).
3. H. Müller, S. Herrmann, C. Braxmaier, S. Schiller, and A. Peters, *Phys. Rev. Lett.* **91**, 020401 (2003).
4. R. K. Shelton, L. S. Ma, H. C. Kapteyn, M. M. Murnane, J. L. Hall, and J. Ye, *Science* **293**, 1286 (2001).
5. S. Chu, *Nature* **416**, 206 (2002).
6. Y. Brenton, M. Kasevich, and S. Chu, in *Atom Interferometry*, P. R. Berman, ed. (Academic, 1997), pp. 363–406.
7. P. Bouyer, T. L. Gustavson, K. G. Haritos, and M. A. Kasevich, *Opt. Lett.* **21**, 1502 (1996).
8. J. Ye and J. L. Hall, *Opt. Lett.* **24**, 1838 (1999).
9. S. Gupta, K. Dieckmann, Z. Hadzibabic, and D. E. Pritchard, *Phys. Rev. Lett.* **89**, 140401 (2002).
10. D. Haubrich and R. Wynands, *Opt. Commun.* **123**, 558 (1996).
11. H. Müller, *Rev. Sci. Instrum.* **76**, 084701 (2005).
12. A. Wicht, J. M. Hensley, E. Sarajlic, and S. Chu, *Phys. Scr. T* **102**, 82 (2002).
13. G. T. Foster, J. B. Fixler, J. M. McGuirk, and M. A. Kasevich, *Opt. Lett.* **27**, 951 (2002).